

# Analysis of the role of O-glycosylation in GH51 $\alpha$ -L-arabinofuranosidase from *Pleurotus ostreatus*

Antonella Amore  
Annabel Serpico  
Angela Amoresano  
Roberto Vinciguerra  
Vincenza Faraco\*

Department of Chemical Sciences, University of Naples "Federico II,"  
Complesso Universitario Monte S. Angelo, via Cinthia, Naples, Italy

## Abstract

In this study, the recombinant  $\alpha$ -L-arabinofuranosidase from the fungus *Pleurotus ostreatus* (rPoAbf) was subjected to site-directed mutagenesis with the aim of elucidating the role of glycosylation on the properties of the enzyme at the level of S160 residue. As a matter of fact, previous mass spectral analyses had led to the localization of a single O-glycosylation at this site. Recombinant expression and characterization of the rPoAbf mutant S160G was therefore performed. It was shown that the catalytic properties are slightly changed by the mutation, with a more evident modification of the  $K_{\text{cat}}$  and  $K_{\text{M}}$  toward the synthetic substrate *pN*-glucopyranoside. More importantly, the mutation negatively affected the stability of the enzyme at various pHs and temperatures. Circular dichroism (CD) analyses showed a minimum at 210 nm for wild-type (wt) rPoAbf, typical of the beta-sheets structure,

whereas this minimum is shifted for rPoAbf S160G, suggesting the presence of an unfolded structure. A similar behavior was revealed when wt rPoAbf was enzymatically deglycosylated. CD structural analyses of both the site-directed mutant and the enzymatically deglycosylated wild-type enzyme indicate a role of the glycosylation at the S160 residue in rPoAbf secondary structure stability. © 2014 The Authors. *Biotechnology and Applied Biochemistry* published by Wiley Periodicals, Inc. on behalf of the International Union of Biochemistry and Molecular Biology, Inc. Volume 62, Number 6, Pages 727–737, 2015

This is an open access article under the terms of the Creative Commons Attribution-NonCommercial-NoDerivs License, which permits use and distribution in any medium, provided the original work is properly cited, the use is non-commercial and no modifications or adaptations are made.

**Keywords:** arabinofuranosidase, fungus, glycosylation, lignocelluloses, site-directed mutagenesis

## 1. Introduction

The enzymes  $\alpha$ -L-arabinofuranosidases (EC 3.2.1.55) act synergistically with other enzymes to allow the complete hydrolysis of hemicelluloses, such as arabinoxytan, arabinogalactan, and

L-arabinan, removing arabinose substituent by the cleavage of the  $\alpha$ -L-arabinofuranosidic linkages [1].

There is a growing interest into  $\alpha$ -L-arabinofuranosidases because of their application as components of the enzymatic cocktail for hydrolysis of pretreated lignocellulose into fermentable sugars for the second-generation ethanol production [2].

According to CAZY classification (Carbohydrate Active enZYmes, <http://www.cazy.org/>) [3], catalytic cores of  $\alpha$ -L-arabinofuranosidases belong to GH3, 43, 51, 54, and 62 families. They are able to hydrolyze terminal nonreducing  $\alpha$ -L-1,2-,  $\alpha$ -L-1,3-, and  $\alpha$ -L-1,5-arabinofuranosyl residues. It is possible to distinguish the following three different classes of arabinofuranosidases: type A  $\alpha$ -L-arabinofuranosidases, acting on short oligosaccharides; type B  $\alpha$ -L-arabinofuranosidases, which is able to hydrolyze side-chain arabinose residues from polymeric substrates; type C  $\alpha$ -L-arabinofuranosidases, which is specific for arabinoxylans and not able to hydrolyze the synthetic substrate *p*-nitrophenyl  $\alpha$ -L-arabinofuranoside (*pNPA*), different from the former types.

Enzymes from the above-mentioned three classes have been found in culture supernatant of various fungi. An

**Abbreviations:** ACN, acetonitrile; CAZY, carbohydrate active enzymes; CBM, carbohydrate-binding module; CD, circular dichroism; GH, Glycoside hydrolase; HPLC, high performance liquid chromatography; MALDI, matrix-assisted laser desorption/ionization; MS/MS, tandem mass spectrometry; MS, mass spectrometry; *pNPA*, *p*-nitrophenyl  $\alpha$ -L-arabinofuranoside; PoAbf,  $\alpha$ -L-arabinofuranosidase produced by the fungus *Pleurotus ostreatus*; rPoAbf, recombinant PoAbf; TOF, time of flight; wt, wild-type.

\*Address for correspondence: Professor Vincenza Faraco, Department of Chemical Sciences, University of Naples "Federico II," Complesso Universitario Monte S. Angelo, via Cintia, 4 80126 Napoli, Italy. Tel.: +39 081 674315; Fax: +39 081 674313; e-mail: vfaraco@unina.it.

Received 13 August 2014; accepted 25 November 2014

DOI: 10.1002/bab.1325

Published online 20 May 2015 in Wiley Online Library

(wileyonlinelibrary.com)

$\alpha$ -L-arabinofuranosidase produced by the fungus *Pleurotus ostreatus* (PoAbf) during solid-state fermentation on tomato pomace was identified and the corresponding gene (*poabf*) and cDNA were cloned and sequenced [4]. On the basis of similarities analysis, the enzyme encoded by *poabf* was classified as a family 51 glycoside hydrolase. Heterologous recombinant expression of PoAbf was carried out in the yeasts *Kluyveromyces lactis* and *Pichia pastoris*, the latter being the best host (180 mg of recombinant protein L<sup>-1</sup> of culture broth). rPoAbf is highly specific for  $\alpha$ -L-arabinofuranosyl linkages and it is worth noting that the enzyme shows very high activity's durability in a broad range of pH. Mass spectral analyses indicated that rPoAbf does not show N-glycosylation. On the other hand, these analyses led to the localization of a single O-glycosylation site at the level of S160.

To elucidate the role of the glycosylation on the properties of rPoAbf, design and preparation of the mutant S160G was carried out in this work by carrying out its recombinant expression and characterization of the recombinant mutant. In addition, wild-type (wt) rPoAbf was treated with an O-glycosidase to further demonstrate the importance of glycosylation for the enzyme structural stability.

## 2. Materials and Methods

### 2.1. Preparation and recombinant expression of the site-directed mutant rPoAbf S160G

The pPICZ-abf containing the cDNA encoding PoAbf (EMBL Data Library, accession number HE565356) was used for recombinant expression in *P. pastoris* as previously reported [4]. Site-directed mutagenesis was performed using the QuikChange site-directed mutagenesis kit (Stratagene, La Jolla, CA, USA) and the pPICZ-abf as a template. The following adopted mutagenic primers are reported, with the mutated nucleotides underlined and bold:

fw: GAACCACTTCTGGT**GG**CACTATCGTTTCCC  
rev: GGGAAACGATAGT**GCC**ACCAGAAGTGGTTC

The mutated gene was sequenced to confirm that only the desired mutations were inserted. The wild-type and mutated enzymes were overexpressed, purified, and assayed as previously described [4]. The activity was measured by the spectrophotometric method with *p*NPA (Gold Biotechnology, St. Louis, MO, USA) as substrate, as previously described [4].

### 2.2. rPoAbf enzymatic deglycosylation and its mass spectrometry analysis

The enzymatic deglycosylation was performed by using O-glycosidase from *Streptococcus pneumoniae*, recombinantly expressed in *Escherichia coli* (Sigma, St. Louis, MO, USA), following a protocol adapted from the supplier's instruction. Two microliters of O-glycosidase was added to 100  $\mu$ g rPoAbf and incubated at 37 °C for 1 H. Fraction containing protein was lyophilized and then dissolved in denaturant buffer (Tris

300 mM pH 8.8, urea 6 M, EDTA 10 mM). Disulfide bridges were reduced with dithiothreitol (10-fold molar excess on the Cys residues) at 37 °C for 2 H, and then alkylated by adding iodoacetamide (fivefold molar excess on thiol residues) at room temperature for 30 Min in the dark. Protein sample was desalted by size exclusion chromatography on a Shephadex G-25M column (GE Healthcare, Uppsala, Sweden). Fractions containing protein were lyophilized and then dissolved in 10 mM AMBIC buffer (pH 8.0). Enzyme digestion was performed using trypsin with an enzyme/substrate ratio of 1:50 (w/w) at 37 °C for 16 H.

The peptide mixture was filtered by using a 0.22  $\mu$ m PVDF membrane (Millipore, Billerica, MA, USA) and analyzed using a 6520 Accurate-Mass Q-TOF (time-of-flight) LC-MS system (Agilent Technologies, Palo Alto, CA, USA) equipped with a 1200 HPLC system and chip cube (Agilent Technologies). The peptide mixture was first concentrated and washed on a 40-nL enrichment column (Agilent Technologies), with 0.1% formic acid (J.T. Backer, Phillipsburg, NJ, USA) in 2% acetonitrile (J.T. Backer) as the eluent. The sample was then fractionated on a C18 reverse-phase capillary column (Agilent Technologies) at a flow rate of 400 nL/Min, with a linear gradient of eluent B (0.1% formic acid in 95% acetonitrile [ACN]) in A (0.1% formic acid in 2% acetonitrile) from 7% to 80% in 50 Min. Peptide analysis was performed using data-dependent acquisition of one MS scan (mass range from 300 to 1,800 *m/z*) followed by tandem mass spectrometry (MS/MS) scan of the five most abundant ions in each MS scan. MS/MS spectra were measured automatically when the MS signal surpassed the threshold of 50,000 counts.

Double- and triple-charged ions were preferably isolated and fragmented over single-charged ions. The acquired MS/MS spectra were transformed in *mzData* (.XML) format and used for protein identification with a licensed version of MASCOT software (www.matrixscience.com) version 2.4.0.

Raw data from nano-LC-MS/MS analysis were used to query the NCBI database NCBI nr 20121120 (21,582,400 sequences; 7,401,135,489 residues), with taxonomy restriction to *Fungi* (1,569,912 sequences). Mascot search parameters were as follows: trypsin as enzyme; three as the allowed number of missed cleavages; carboamidomethyl as fixed modification; oxidation of methionine; pyro-Glu N-term Q as variable modifications; 10 ppm MS tolerance and 0.6 Da MS/MS tolerance; and peptide charge from +2 to +3. Peptide score threshold provided from MASCOT software to evaluate quality of matches for MS/MS data was 25. Spectra with MASCOT score of <25 having low quality were rejected.

Matrix-assisted laser desorption/ionization – Mass Spectrometry (MALDI-MS) experiments were performed on a Voyager-DE STR MALDI-TOF mass spectrometer (Applied Biosystems, Framingham, MA, USA) equipped with a nitrogen laser (337 nm). Of the total mixture, 1  $\mu$ L was mixed (1:1, v/v) with a solution of 10 mg/mL  $\alpha$ -cyano-4-hydroxycinnamic acid in ACN/citrate buffer (70:30, v/v). Spectra were acquired using a mass (*m/z*) range of 500–4,000 amu.

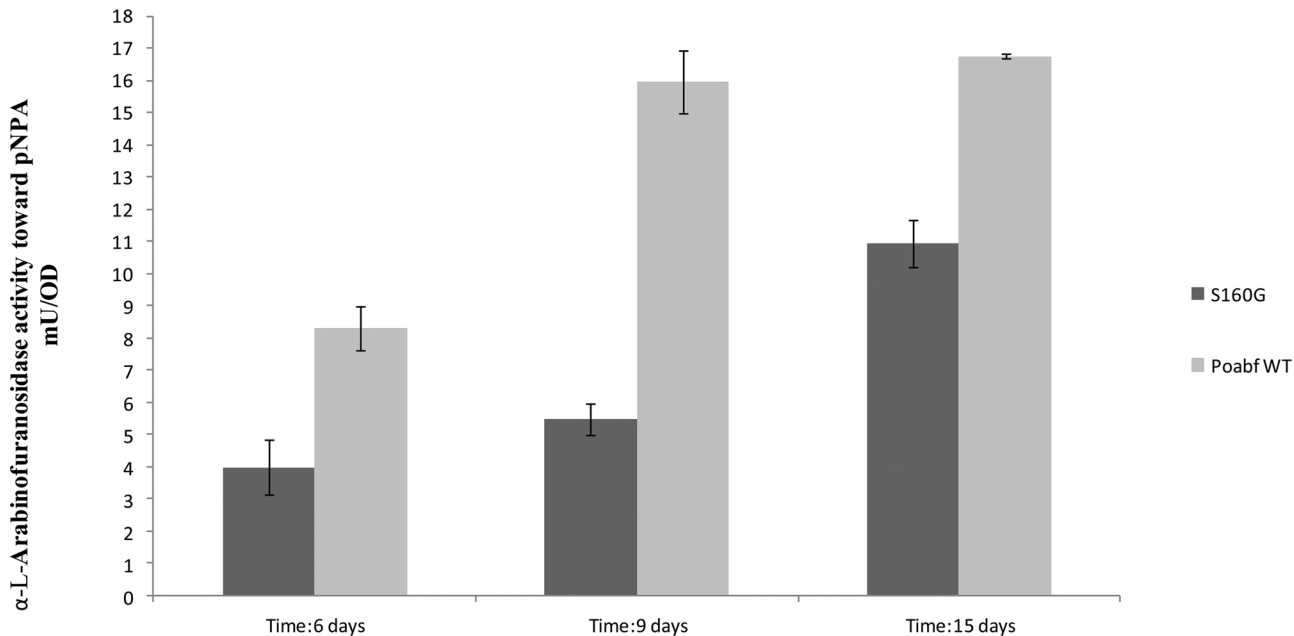


**FIG. 1**

Time course of arabinofuranosidase activity/s production by rPoAbf and rPoAbf S160G at 20 °C.

### 2.3. Optimum temperature and temperature resistance

The optimum temperature of the purified enzyme mutant rPoAbf S160G was determined in comparison with that of the wild-type enzyme, assaying the activity toward pNPA at 30, 40, 50, and 60 °C, as previously described [4]. The temperature resistance of rPoAbf S160G was investigated in comparison with the wild-type enzyme by incubating the purified enzyme preparation at 30, 40, 50, and 60 °C, as previously described [4]. The samples withdrawn were assayed for residual  $\alpha$ -arabinosidase activity performing incubation (10 Min) at 40 °C. The experiments were performed in duplicate and reported values are representative of three experiments.

### 2.4. Optimum pH and pH stability

The optimum pH of the purified enzyme mutant rPoAbf S160G was determined in comparison with that of the wild-type enzyme, using the substrate of the activity assay (2 mM pNPA) dissolved in citrate phosphate buffers [5] with pH values between 3.0 and 7.0 and in 50 mM Tris-HCl with pH values between 7.0 and 8.0, as previously described [4]. The pH stability of the purified rPoAbf S160G preparation was studied in comparison with the wild-type enzyme by diluting the enzyme preparation in citrate phosphate buffers, pH 3–8, and incubating it at 25 °C, as previously described [4]. The experiments were performed in duplicate and reported values are representative of three experiments.

### 2.5. Assays of enzyme specificity

The activity of rPoAbf S160G was assayed against the substrates pNPA, pNP- $\beta$ -D-xylopyranoside, pNP- $\alpha$ -D-glucopyranoside,

pNP- $\beta$ -D-glucopyranoside, and oNP- $\beta$ -D-galactopyranoside (all purchased from Carbosynth, Berkshire, UK), at concentrations ranging from 0.1 to 6 mM in citrate phosphate buffer (pH 5) [5]. The activity against the natural substrates CM-linear arabinan and larch arabinogalactan and the arabinooligosaccharides 1,5- $\alpha$ -arabinotriose and 1,5- $\alpha$ -arabinohexaose (Megazyme International Ireland, Co. Wicklow, Ireland) was also assayed by measuring the liberation of arabinose using the D-galactose/lactose kit (Megazyme International Ireland, Co.), following the manufacturer's instructions. rPoAbf S160G (350 mU, measured on pNPA) was incubated with 0.2% arabinans in 100 mM sodium acetate buffer (pH 4.6) at 37 °C for 72 H (final volume 300  $\mu$ L). Arabinooligosaccharides were dissolved in 100 mM sodium acetate buffer (pH 4.6) and incubated with 7 mU (measured on pNPA) of rPoAbf S160G at 37 °C for 1 H (final volume 300  $\mu$ L). The activity of the mutant against the substrate AZO-wheat arabinoxylan (Megazyme International Ireland, Co.) was assayed following supplier's instructions.

The experiments were performed in duplicate and reported values are representative of three experiments.

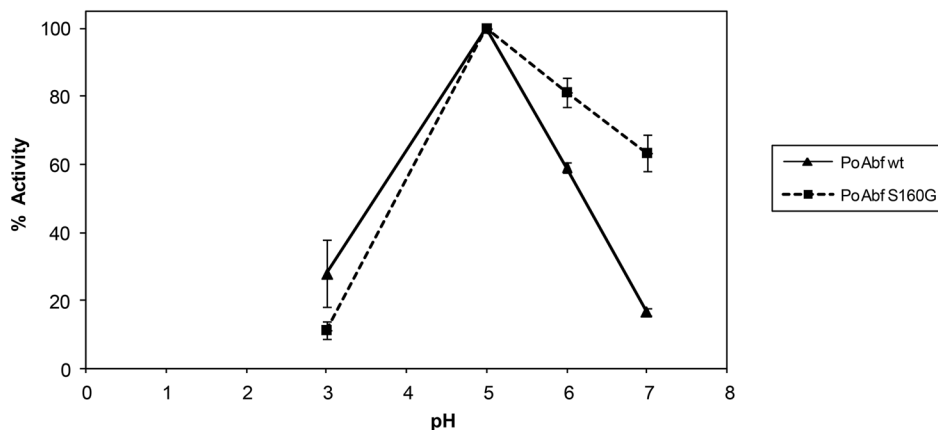
### 2.6. Determination of $k_{cat}$ and $K_M$

The Michaelis–Menten constants  $K_M$  and  $k_{cat}$  were determined, performing the activity assay with a pNPA concentration in the range from 0.1 to 2.0 mM (pH 5.0) at 40 °C for 10 Min. The experiments were performed in duplicate and reported values are representative of three experiments.

### 2.7. Spectroscopy techniques

Far-UV circular dichroism (CD) spectra were recorded on a Jasco J715 spectropolarimeter equipped with a Peltier thermostatic cell holder in a quartz cell (0.1 cm light path) from 190 to 250 nm. The temperature was kept at 25 °C and the

a



b

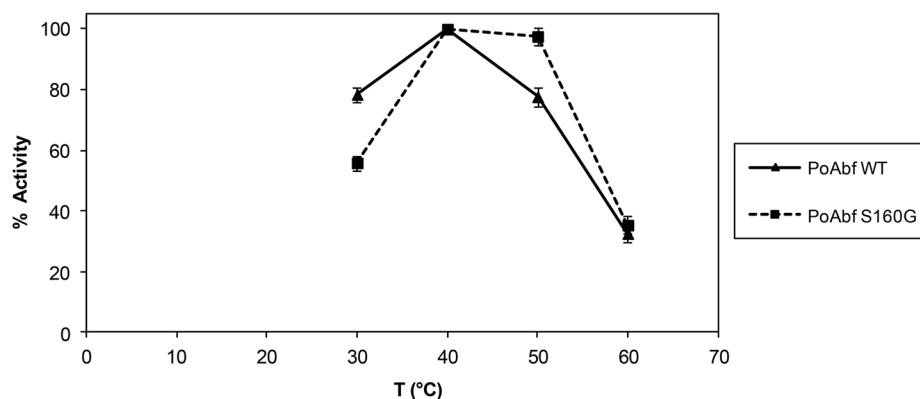


**FIG. 2**

Effect of pH (a) and temperature (b) on the activity of rPoAbf and rPoAbf S160G toward pNPA as a substrate. The percentage of activity reported in (a) and (b) was calculated as ratio to the maximum activity measured at optimal pH of 5 and temperature of 40 °C.

sample compartment was continuously flushed with nitrogen gas. The final spectra were obtained by averaging three scans, using a bandwidth of 1 nm, a step width of 0.5 nm and a 4 Sec averaging per point.

The spectra were then corrected for the background signal using a reference solution without the protein.

## 3. Results

### 3.1. Production of rPoAbf S160G mutant

Mass spectral analyses had indicated that the  $\alpha$ -L-arabinofuranosidase from the fungus *P. ostreatus* expressed in *P. pastoris* (rPoAbf) exhibits O-glycosylation at the level of

S160, whereas it does not show N-glycosylation. To elucidate the role of the glycosylation on the properties of rPoAbf, design and preparation of the mutant rPoAbf S160G were carried out in this work by setting up a recombinant expression system of the mutant for its characterization. The production of rPoAbf S160G mutant by *P. pastoris* was analyzed in comparison with that of wt rPoAbf at 20 °C, this being the optimal temperature for the production of the wild-type enzyme [4]. As shown in Fig. 1, rPoAbf S160G mutant levels of production are lower than those achieved for the wild-type enzyme, even if this difference decreases at longer times.

### 3.2. Characterization of the mutant rPoAbf S160G

#### Catalytic properties

rPoAbf S160G was purified and characterized for its catalytic properties in comparison with the wild type. It follows Michaelis–Menten kinetics when incubated with pNPA, with a  $K_M$  of  $0.89 \pm 0.19$  mM and a  $k_{cat}$  of  $2,590 \pm 165$  Min<sup>-1</sup>, different from the wild-type enzyme for this substrate having a  $K_M$  of  $0.64 \pm 0.11$  mM and a  $k_{cat}$  of  $3,010 \pm 145$  Min<sup>-1</sup>.

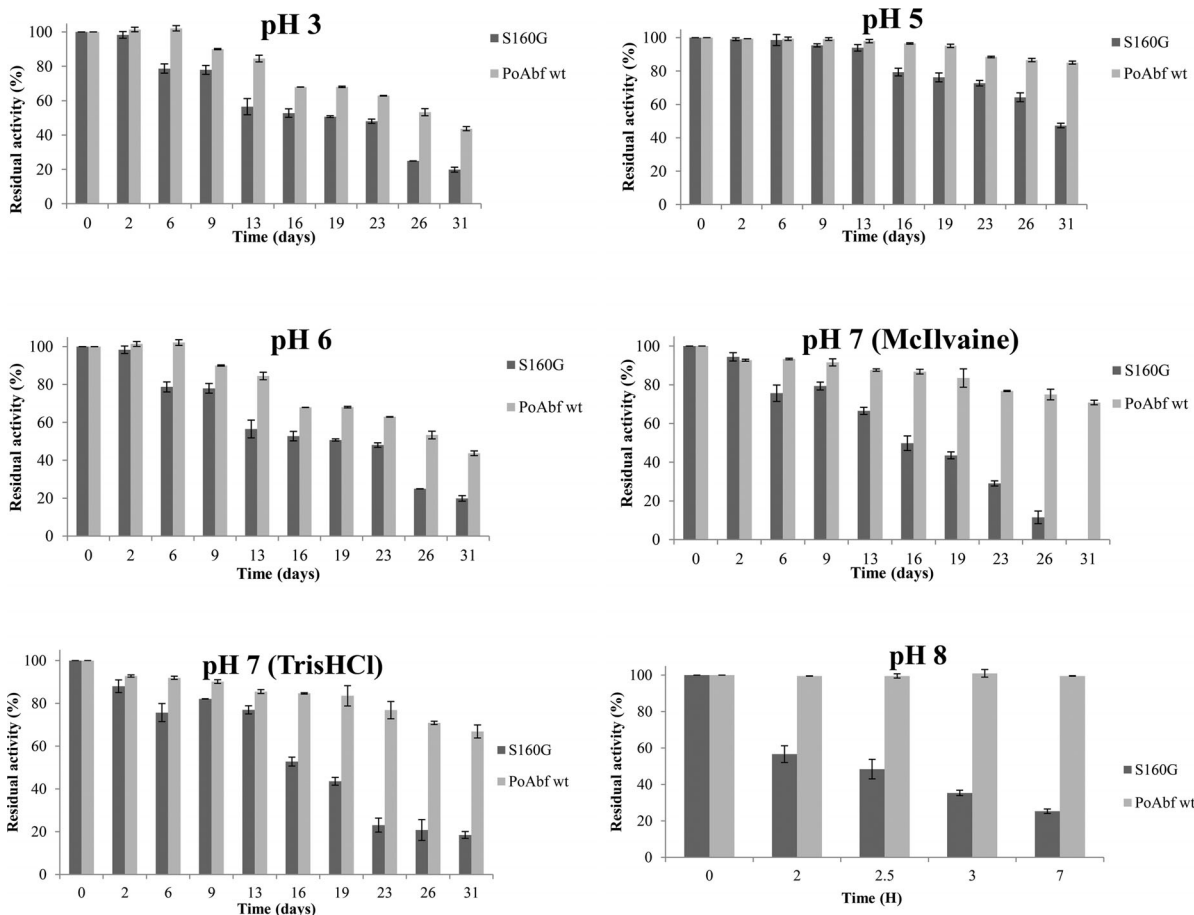


**FIG. 3**

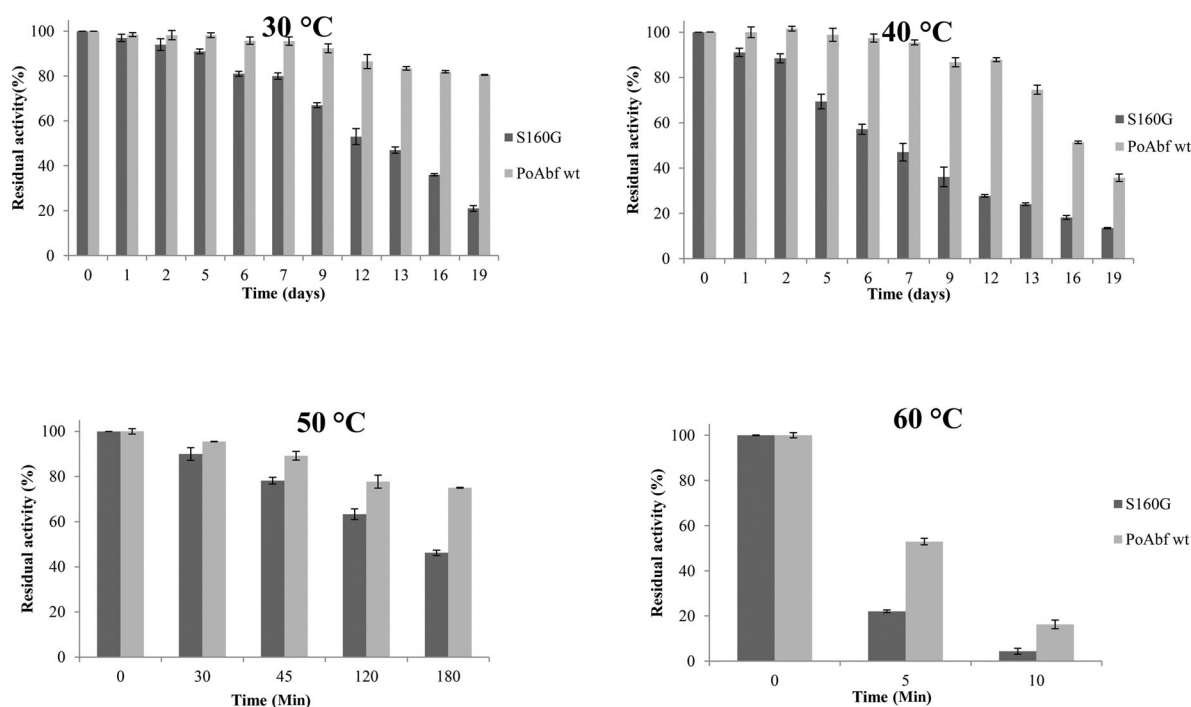
*pH resistance of rPoAbf and rPoAbf S160G.*

Optimum pH and optimal temperature values for the enzymatic reaction of rPoAbf S160G were estimated to be 5 and 40 °C, respectively, similarly to the case of the wild-type enzyme (Fig. 2). The main difference between the two analyzed enzymes is that the mutant shows an optimal catalytic performance also at 50 °C, showing an activity percentage that is 1.24-fold higher than that of the wild-type enzyme. Moreover, the mutant shows an activity percentage 1.37- and 3.7-fold higher than that of the wild type, when assayed toward *p*NP-arabinofuranoside, at pH 6 and 7, respectively.

On the other hand, it was demonstrated that the mutation S160G negatively affects the resistance of rPoAbf at all the tested values of pH (Fig. 3) and temperature (Fig. 4), especially at 40 °C ( $t_{1/2}$  wt = 16 days;  $t_{1/2}$  S160G = 7 days), 50 °C ( $t_{1/2}$  wt = 17 H;  $t_{1/2}$  S160G = 3 H), pH 5 ( $t_{1/2}$  wt = 51 days;  $t_{1/2}$  S160G = 31 days), pH 7 citrate-phosphate buffer ( $t_{1/2}$  wt = 38 days;  $t_{1/2}$  S160G = 16 days), pH 7 Tris-HCl buffer ( $t_{1/2}$  wt = 42 days;  $t_{1/2}$  S160G = 16 days), and pH 8 ( $t_{1/2}$  wt = 38 days;  $t_{1/2}$  S160G = 2.5 H), where a strong reduction in the half-life of the mutant in comparison with the wild-type enzyme was observed.

The mutant was shown to be able to hydrolyze both the tested arabinooligosaccharides 1,5- $\alpha$ -arabinotriose and 1,5- $\alpha$ -arabinohexaose, with an efficiency similar to that of the wild-type enzyme (Table 1). rPoAbf S160G showed a behavior similar to the wild type also toward CM-linear arabinan and larch arabinogalactan (Table 1). Moreover, when 75 mU of the S160G mutant was incubated with the AZO-wheat arabinoxylan, it was shown to possess an endo-1,4- $\beta$ -xylanase activity of around  $0.60 \pm 0.02$  U mL<sup>-1</sup>, similarly to the activity of the corresponding amount of the wild-type enzyme ( $0.63 \pm 0.03$  U mL<sup>-1</sup>). Thus, glycosylation does not affect the hydrolytic ability of rPoAbf on these substrates.

When the hydrolyzing ability of rPoAbf S160G was tested versus a series of other nitrophenyl glycosides (*p*NP- $\beta$ -D-xylopyranoside, *p*NP- $\alpha$ -D-glucopyranoside, *p*NP- $\beta$ -D-glucopyranoside, and *o*NP- $\beta$ -D-galactopyranoside), it was shown that only *p*NP- $\beta$ -D-glucopyranoside was recognized by the mutated enzyme similarly to the wild type. Toward this substrate, a difference in catalytic performances was revealed because the mutant showed to have a  $K_M$  of  $5.03 \pm 0.12$  mM (wt =  $4.07 \pm 0.15$  mM) and a  $k_{cat}$  of  $23.0 \pm 0.9$  Min<sup>-1</sup>, the latter being around 100% higher than the value measured for the wild type ( $11.0 \pm 0.6$  Min<sup>-1</sup>).


**FIG. 4**

Thermoresistance of rPoAbf and rPoAbf S160G.

### Structural properties

Protein aliquot was reduced and carboxyamidomethylated as described before and subjected to enzymatic digestion by using trypsin as a proteolytic enzyme. Thus, the peptide mixture was fractionated by microfluidic capillary high-performance liquid chromatography-mass spectrometry (HPLC) analysis, and directly analyzed by MS/MS, producing daughter ion spectra from which sequence information on individual peptides was obtained. This information was sufficient to unambiguously identify the protein. As a whole, mass spectral analyses allowed to confirm the primary structure of the  $\alpha$ -L-arabinofuranosidase (NCBI nr ID GI:340003220) from *P. ostreatus*, with a percentage of total amino acid sequence of 24%, as summarized in Table 2. In addition, a manual interpretation of the MS/MS spectrum obtained in a data-dependent acquisition mode demonstrated the presence of a single amino acid mutation within peptide sequence, resulting in the desired substitution S160G. In Fig. 5, the fragmentation spectrum of the doubly charged ion 758.9214  $m/z$  is reported.

CD analyses were also performed to study and compare the structure of wt rPoAbf and its mutant S160G (Fig. 6a).

Spectra between 190 and 250 nm were recorded, showing a minimum at 210 nm for wt PoAbf, typical of the beta-sheets structure. As far as PoAbf S160G is concerned, this minimum is shifted, suggesting the presence of an unfolded structure. Particularly, for the mutant, an increase in the unfolded structure content (from 36% to 44%) and a decrease in the beta-sheet structure content (from 35% to 24%) were recorded

**TABLE 1**

Arabinose liberation from natural substrates and arabinooligosaccharides

| Substrate             | Amount of released sugar ( $\mu\text{g/mL}$ ) wild type | Amount of released sugar ( $\mu\text{g/mL}$ ) S160G |
|-----------------------|---|---|
| Larch arabinogalactan | 9.09 $\pm$ 0.56   | 6.84 $\pm$ 1.33                                     |
| CM-linear arabinan    | 249.25 $\pm$ 7.64                                       | 250.32 $\pm$ 4.61                                   |
| Arabinotriose         | 112.26 $\pm$ 3.35                                       | 97.87 $\pm$ 2.47                                    |
| Arabinohexaose        | 105.00 $\pm$ 7.77                                       | 102.02 $\pm$ 4.75                                   |

Equivalents of galactose were measured as described in the section Material and Methods.

by using the software Dichroweb [6, 7], suggesting a role of the glycosylation in rPoAbf secondary structure stability.

### 3.3. Characterization of the enzymatically deglycosylated rPoAbf

To further demonstrate the importance of glycosylation for the enzyme structural stability, an enzymatic deglycosylation of wt rPoAbf was carried out with a commercial O-glycosidase. It was shown that this enzymatic treatment negatively affected rPoAbf activity, with a loss of activity of around 50%. After deglycosylation, rPoAbf was reduced and alkylated and digested as described before for mass spectral analyses. The absence of

| <b>TABLE 2</b> LC-MS/MS analysis of the rPoAbf digested with trypsin |            |                        |                       |
|--|------------|------------------------|-----------------------|
| Peptide  | <i>m/z</i> | <i>MH</i> <sup>+</sup> | Sequence              |
| 104–110  | 374.2115   | 2                      | FTVPAGR               |
| 126–133  | 434.7426   | 2                      | IVASSTYK              |
| 526–533  | 465.2406   | 2                      | SASYFVQK              |
| 562–571  | 530.3070   | 2                      | NTATGEIIIK            |
| 383–391  | 537.2984   | 2                      | WPAFVNALR             |
| 552–561  | 548.2838   | 2                      | TGTAFWGVTR            |
| 231–243  | 701.8669   | 2                      | DDIATALAEMKPK         |
| 231–244<br>+OxidizedMet  | 709.8633   | 2                      | DDIATALAEMKPK         |
| 111–125  | 774.3698   | 2                      | TGQVGFANSGFFGMK       |
| 111–126<br>+OxidizedMet  | 782.3710   | 2                      | TGQVGFANSGFFGMK       |
| 247–261  | 793.9026   | 2                      | FPGGNNLEGQTVPTR       |
| 171–186  | 859.4476   | 2                      | GASTSWQQISVSLTPR      |
| 534–551  | 1,013.9991 | 2                      | LFSTNMGNEYIPSTLPSR    |
| 534–552<br>+OxidizedMet  | 1,021.9996 | 2                      | LFSTNMGNEYIPSTLPSR    |
| 224–261  | 679.6828   | 3                      | FFRFPGGNNLEGQTVPTR    |
| 469–489  | 761.0116   | 3                      | LTFSTMQSASGEAAYMIGMER |

O-glycosylation due to the action of the enzyme O-glycosidase was confirmed by MALDI–MS analyses (Table 3). Figure 7 reports the MALDI–MS spectrum obtained from the analysis of the tryptic peptides mixture of deglycosylated rPoAbf, showing the presence of a signal at *m/z* 1,546.51 assigned to the unmodified peptide <sup>156</sup>TTSGSTIVSQTVP<sup>170</sup>. On the other hand, the peptide fragment at *m/z* 1,911.51 previously detected [4] and attributed to the peptide carrying a GalNacHex oligosaccharide moiety was not detected. Thus, no glycosylation at the level of Ser160 was inferred. The effect of the enzymatic deglycosylation on rPoAbf secondary structures was studied by CD analyses. Interestingly, a partial unfolding structure (Fig. 6b) was also observed in this case, thus contributing to confirm the role of O-glycosylation in the stability of the secondary structure of rPoAbf.

## 4. Discussion

Glycosylation is one of the most common and important post-translational modifications of proteins, which is known to play an essential role in the function, the structural folding, and the stability. Two major types of glycosylation, N- and O-linked, are frequently observed in fungal glycoside hydrolases and both types of glycosylation were proposed to impact the catalytic efficiency and the stability of glycoside hydrolases. Zhou et al. [8] computationally annotated the glycosylated residues in all known cellulases and conducted a systematic analysis of the distributions of the N- and O-linked glycosylated residues in these enzymes.

Glycosylation strongly affects the cellulose binding affinity in cellulases [9]. The study of the glycosylation pathways of glycoside hydrolases is necessary in view of their overproduction by mean of recombinant expression. Glycosylation of glycosyl hydrolases (GHs) varies with the recombinant expression host

**TABLE 3** MALDI–MS analysis of the rPoAbf digested with trypsin after deglycosylation with O-glycosidase enzymes

| <i>m/z</i>              | Peptide     | Sequence  |
|-------------------------|-------------|---|
| 747.25                  | F[104–110]R | FTVPAGR   |
| 1,073.36                | W[383–391]  | WPAFVNALR                                       |
| 1,546.51 (unmodified)   | T[156–170]R | TTSGSTIVSQTVP <sup>170</sup>                    |
| 1,586.45                | F[247–261]R | FPGGNNLEGQTVPTR                                 |
| 2,026.57                | L[534–551]R | LFSTNMGNEYIPSTLPSR                              |
| 2,043.52 + Oxidized Met | L[534–551]R | LFSTNMGNEYIPSTLPSR                              |
| 2,280.58                | L[469–489]R | LTFSTMQSASGEAAYMIGMER                           |
| 2,396.81                | T[111–133]K | TGQVGFANSGFFGMKIVASSTYK                         |
| 2,962.70                | N[441–468]R | NGVTFEAGEYAAISTNPNDIFGSPANGR                    |
| 3,246.00                | T[156–186]R | TTSGSTIVSQTVP <sup>170</sup> IRGASTSWQQISVSLTPR |

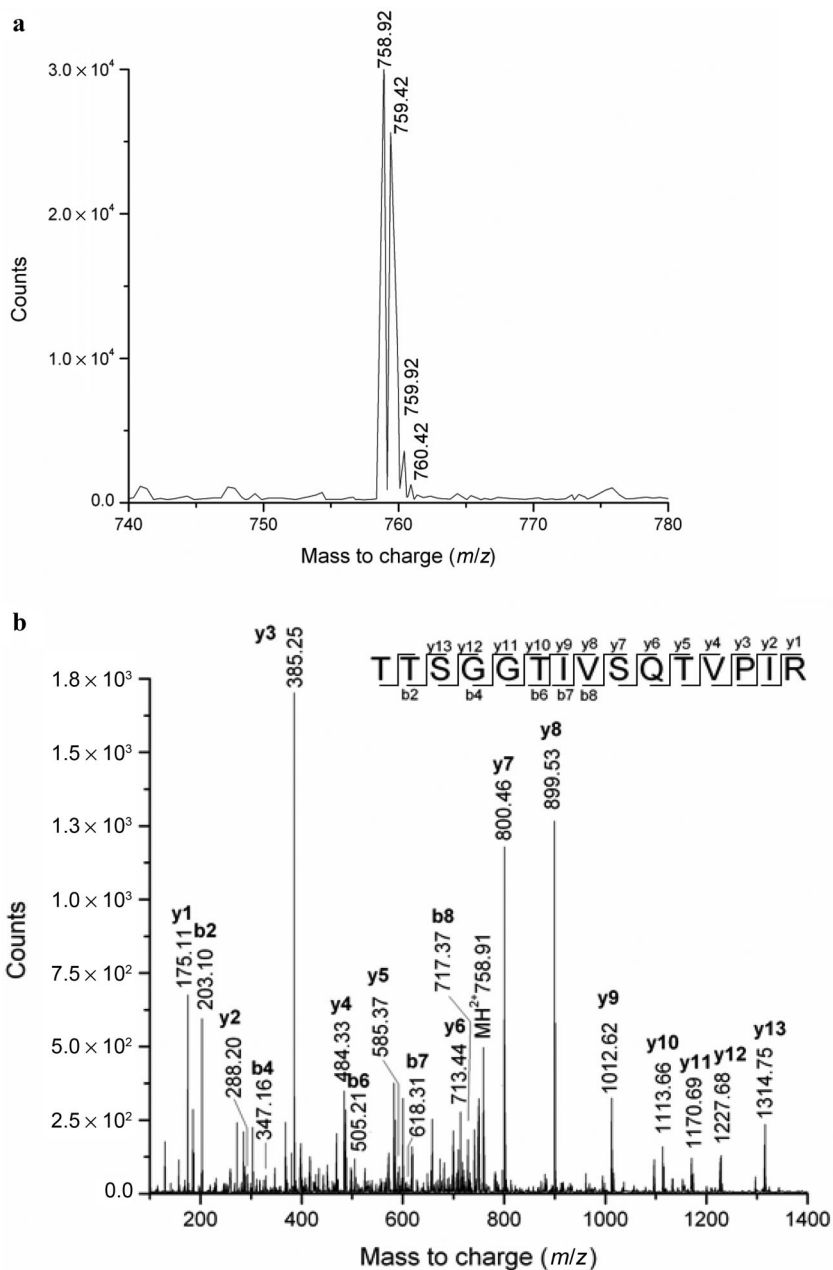


**FIG. 5**

Doubly charged ion 758.92 m/z spectrum (a) and its relative MS/MS spectrum (b).

and the culture conditions. Thus, it is important to study the chemical nature of the glycans that decorate the fungal glycoside hydrolases to investigate their effect on cellulose and hemicellulose conversion.

Few studies have so far deeply investigated the effect of glycosylation on the GH families involved in lignocellulosic biomass degradation [9]. In most of the cases, an approach “all or nothing” has been followed studying only the effect of the complete deglycosylation and not performing the partial removal of glycan moiety or its composition modification. This

makes the role of glycosylation in these classes of enzymes still poorly understood [10].

Most fungal cellulases are characterized by the presence of O-glycans at the level of the linker peptide between GH and carbohydrate-binding module (CBM) domains. On the other hand, the carbohydrate domains are mostly decorated with N-glycans, whose effects cannot be always easily predicted [10].

As reported by Jeoh et al. [11], most of the *Trichoderma reesei* cellulases are glycoproteins, where the extent and type of glycans can strongly vary. The most extensive studies have been performed on the cellulase Cel7A, which carries a highly glycosylated O-linked linker peptide between its GH and CBM domains. For this cellulase, an altered level of N-linked



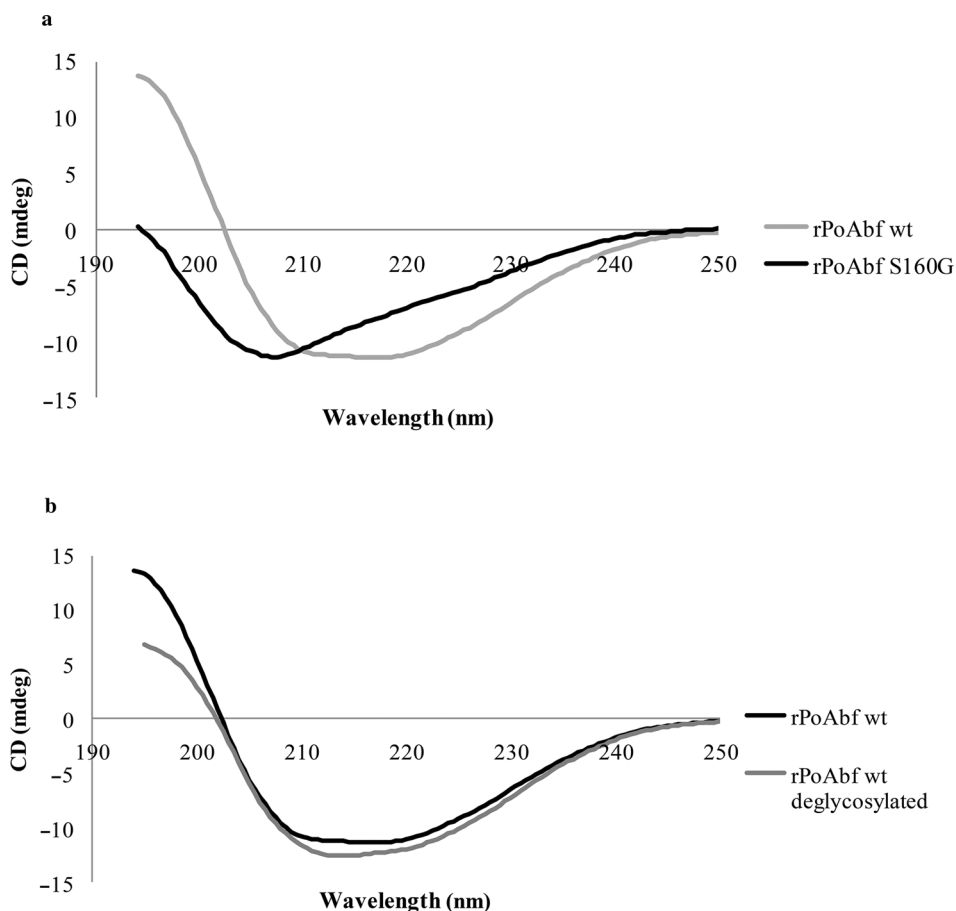


**FIG. 6** (a) CD spectra of wt rPoAbf and the mutant rPoAbf S160G and (b) CD spectra of enzymatically O-deglycosylated wt rPoAbf and rPoAbf.

glycosylation was observed to negatively impact the activity and the cellulose binding affinity. In particular, comparing the performances of the native Cel7 enzyme with those of the rCel7A recombinantly produced in the fungus *Aspergillus niger* var. *awamori*, it was observed that the increased level of N-glycosylation reduces the activity and increases the non-productive binding on cellulose. After treatment with the N-glycosidase PNGaseF, the molecular weight of the recombinant enzyme approached to that of the commercial enzyme and the activity on cellulose was improved. Beckham et al. [12] deeply studied the Cel7A linker peptide in solution, with and without the glycosylation, demonstrating that the primary effect of the glycosylation is to extend the most thermodynamically stable value of the operating distance for the linker from 37 to 53Å. On the other hand, Payne et al. [13] demonstrated that both N- and O-linked glycans on the carbohydrate domain of Cel6A do not affect either the energetics of the protein and ligand interactions or the fluctuation of the ligand in the enzyme tunnel.

Very recently, Chen et al. [14] studied the effect of O-mannosylation on the stability and cellulose binding affinity of family 1 CBMs. Particularly, they produced a collection of

glycoforms and demonstrated that O-linked mannose residues increase the proteolytic stability of the CBM in a glycan size-dependent manner. Moreover, the O-mannose glycosylation positively affects the thermostability in accord to the results achieved in this work where the absence of the O-glycosylation site corresponds to a decrease in thermostability of the enzyme rPoAbf.

The effect of N-linked glycosylation on secretion, activity, and stability of alpha-amylase from *Aspergillus oryzae* was studied by Eriksen et al. [15], showing that deglycosylation did not lead to the loss of enzyme stability. The  $\alpha$ -L-arabinofuranosidase 54 from *Aspergillus kawachii* was shown to possess two N-linked glycosylation sites in the catalytic domain. The biochemical properties and kinetic parameters of the enzymes were studied after replacing Asn83, Asn202, and the two residues together with glutamine. The N83Q mutant enzyme had the same catalytic activity and thermostability as the wild-type enzyme, whereas the N202Q and N83Q/N202Q mutant enzymes exhibited a considerable decrease in thermostability and a slightly lower specific activity toward arabinan and debranched arabinan, compared with the glycosylated wild-type enzyme, thus suggesting that the glycosylation at Asn202 may contribute to thermostability and catalysis [16]. The effect of glycosylation on the thermostability of a GH family 10 xylanase produced by *Thermopolyspora flexuosa* was investigated by Anbarasan et al. [17], showing that

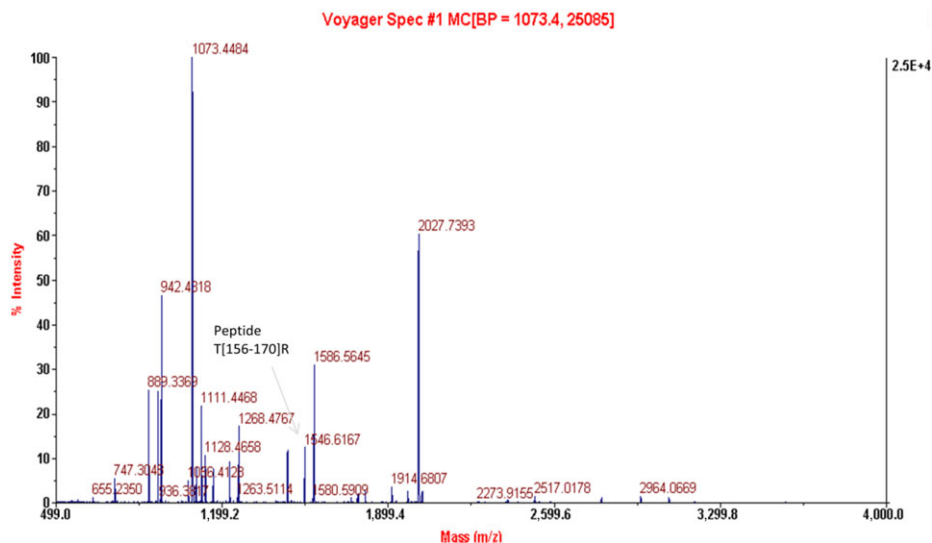


**FIG. 7**

MALDI-MS spectrum obtained from the analysis of the tryptic peptide mixture of deglycosylated rPoAbf.

glycosylation at Asn26, located in an exposed loop, decreased the thermostability of the xylanase.

Interestingly, the results achieved by Taylor et al. [18] through computational analyses demonstrated the importance of CBM glycosylation on the enzyme binding affinity of a family 1 CBM.

All the mentioned studies suggested the importance of a new approach for glycoside hydrolases production that, based on modification of glycosylation patterns by heterologous expression, manipulation of culture conditions, or introduction of artificial glycosylation sites, can improve their performances in lignocelluloses conversion.

Despite the wide differences so far reported in the glycosylation effects on glycoside hydrolases properties, the results achieved in this work confirm the importance of glycosylation for the lignocellulose degrading enzymes.

## 5. Conclusions

Mutational analysis of the O-glycosylation site of GH51  $\alpha$ -L-arabinofuranosidase from *P. ostreatus* (PoAbf) was performed by recombinant expression of the rPoAbf mutant S160G in *P. pastoris* and its characterization, in comparison with the wt rPoAbf. The occurrence of the desired substitution S160G was then confirmed by MS/MS. This study showed that the catalytic properties of this  $\alpha$ -L-arabinofuranosidase are essentially not changed by the mutation. On the other hand, both thermostability and pH resistance were drastically decreased by the mutagenesis at all the tested pH and temperature conditions. CD analyses showed an increase in the unfolded structure content and a decrease in the beta-sheet structure content for both the site-directed mutant and the enzymatically deglycosylated rPoAbf, indicating a role of the glycosylation in

rPoAbf secondary structure stability. The results obtained in this work indicate the importance of studying the glycosylation of glycoside hydrolases, whose catalytic performance has been so far reported to be affected by the presence of glycans at both O- and N-sites.

## 6. Acknowledgements

This work was supported by grant from the Ministero dell'Università e della Ricerca Scientifica, Industrial Research Project "Integrated agro-industrial chains with high energy efficiency for the development of eco-compatible processes of energy and biochemicals production from renewable sources and for the land valorization (EnerbioChem)" PON01\_01966, funded in the frame of Operative National Programme Research and Competitiveness 2007–2013 D. D. Prot. no. 01/Ric. 18.1.2010.

## 7. References

- [1] Shallom, D., and Shoham, Y. (2003) *Curr. Opin. Microbiol.* 6, 219–228.
- [2] Gao, D., Uppugundla, N., Chundawat, S. P. S., Yu, X., Hermanson, S., Gowda, K., Brumm, P., Mead, D., Balan, V., and Dale, B. E. (2011) *Biotechnol. Biofuels* 4, 5.
- [3] Cantarel, B. L., Coutinho, P. M., Rancurel, C., Bernard, T., Lombard, V., and Henrissat, B. (2009) *Nucleic Acids Res.* 37, 233–238.
- [4] Amore, A., Amoresano, A., Birolo, L., Henrissat, B., Leo, G., Palmese, A., and Faraco, V. (2012) *Appl. Microbiol. Biotechnol.* 94, 995–1006.
- [5] McIlvaine, T. C. (1921) *J. Biol. Chem.* 49, 183–186.
- [6] Whitmore, L., and Wallace, B. A. (2004) *Nucleic Acids Res.* 32, 668–673.
- [7] Whitmore, L., and Wallace, B. A. (2008) *Biopolymers* 89, 392–400.
- [8] Zhou, F., Olman, V., and Xu, Y. (2009) *Genomics Proteomics Bioinformatics* 7, 194–199.
- [9] Yang, B., Dai, Z., Ding, S. Y., and Wyman, C. E. (2011) *Biofuels* 2, 421–450.
- [10] Beckham, G., Dai, Z., Matthews, J. F., Momany, M., Payne, C. M., Adney, W. S., Baker, S. E., and Himmel, M. E. (2012) *Curr. Opin. Biotechnol.* 23, 338–345.
- [11] Jeoh, T., Michener, W., Himmel, M. E., Decker, S. R., and Adney, W. S. (2008) *Biotechnol. Biofuels* 1, 10.
- [12] Beckham, G. T., Bombe, Y. J., Matthews, J. F., Taylor, C. B., Resch, M. G., Yarbrough, J. M., Decker, S. R., Bu, L., Zhao, X., McCabe, C., Wohler, J.,

- Bergensträhle, M., Brady, J. W., Adney, W. S., Himmel, M. E., and Crowley, M. F. (2010) *Biophys. J.* 99, 3773–3781.
- [13] Payne, C. M., Bomble, Y. J., Taylor, C. B., McCabe, C., Himmel, M. E., Crowley, M. F., and Beckham, G. T. (2011) *J. Biol. Chem.* 286, 41028–41035.
- [14] Chen, L., Drake, M. R., Resch, M. G., Greene, E. R., Himmel, M. E., Chaffey, P. K., Beckham, G. T., and Tan, Z. (2014) *Proc. Natl. Acad. Sci. USA* 111, 7613.
- [15] Eriksen, S. H., Jensen, B., and Olsen, J. (1998) *Curr. Microbiol.* 37, 117–122.
- [16] Koseki, T., Miwa, Y., Mese, Y., Miyanaga, A., Fushinobu, S., Wakagi, T., Shoun H., Matsuzawa, H., and Hashizume, K. (2006) *Biochim. Biophys. Acta* 1760, 1458–1464.
- [17] Anbarasan, S., Jänis, J., Paloheimo, M., Laitaoja, M., Vuolanto, M., Karimäki, J., Vainiotalo, P., Leisola, M., and Turunen, O. (2010) *Appl. Environ. Microbiol.* 76, 356.
- [18] Taylor, C. B., Talib, M. F., McCabe, C., Bu, L., Adney, W. S., Himmel, M. E., Crowley, M. F., and Beckham, G. T. (2012) *J. Biol. Chem.* 287, 3147–3155.